Deep Velocity Profiling with Self-contained ADCPs

J. FISCHER AND M. VISBECK

Institut für Meereskunde, Kiel, Germany

(Manuscript received 27 October 1992, in final form 8 March 1993)

ABSTRACT

Ocean deep velocity profiles were obtained by lowering a self-contained 153.6-kHz acoustic Doppler current profiler (ADCP) attached to a CTD–rosette sampler. The data were sampled during two *Meteor* cruises in the western tropical Atlantic.

The ADCP depth was determined by integration of the vertical velocity measurements, and the maximum depth of the cast was in good agreement with the CTD depth. Vertical shears were calculated for individual ADCP velocity profiles of 140–300-m range to eliminate the unknown horizontal motion of the instrument package. Subsequent raw shear profiles were then averaged with respect to depth to obtain a mean shear profile and its statistics. Typically, the shear standard deviations were about 10^{-3} s^{-1} when using up and down traces simultaneously.

The shear profiles were then vertically integrated to get relative velocity profiles. Different methods were tested to transform the relative velocities into absolute velocity profiles, and the results were compared with Pegasus dropsonde measurements. The best results were obtained by integrating the raw velocities and relative velocities over the duration of the cast and correcting for the ship drift determined from the Global Positioning System.

Below 1000-m depth a reduction of the measurement range was observed, which results either from a lack of scatterers or instrumental problems at higher pressures.

1. Introduction

Acoustic Doppler technology is now widely used for measuring velocities in the ocean. Ship-mounted acoustic Doppler current profilers (ADCPs) combined with accurate navigation systems such as the Global Positioning System (GPS) are nowadays a common tool to measure currents in the top 300 m of the ocean while the ships are under way (e.g., Joyce et al. 1982). In moored applications, ADCPs have also been used for several years to measure horizontal currents (e.g., Schott 1986), and even vertical velocities were measured during winter convection (Schott et al. 1988; Schott et al. 1993).

Here, we would like to present a method of how an ADCP (self-contained version) can be used to measure deep velocity profiles during standard hydrographic casts. Absolute velocity profiles with sufficient accuracy are difficult to obtain and expensive in consumables and ship time. High-quality velocity profiles can be obtained by acoustically tracked dropsondes like the Pegasus (Spain et al. 1981) or the "White Horse" (Luyten et al. 1982). These systems need transponder arrays at the sea floor with exact knowledge of their three-dimensional position. From our own experience it takes up to 5 h of ship time to survey such a transponder array, and each Pegasus profile down to the 4000-m depth takes another 4 h, which can, however, be combined with a CTD cast. The transponder costs are high, and once deployed, the position of the station cannot be altered unless recoverable transponders are used. The motivation for using an ADCP for deep velocity profiling was therefore threefold: first to increase station flexibility, second to reduce ship time, and finally to cut down on station (transponder) costs.

Firing and Gordon (1990) were the first to use a 300-kHz ADCP in conjunction with a CTD for deep current profiling. Their trials, however, revealed errors of the order 10 cm s^{-1}, much too large to be used for quantitative purposes (e.g., transport calculations). Briefly, their application was to differentiate individual ADCP profiles vertically, then to average overlapping profiles in depth cells and integrate the resulting mean shear profile from a reference level to obtain a relative velocity profile. The depth of the instrument package was determined by integrating the measured vertical velocity (lowering speed) in time. We extended this method by carefully testing the data quality and eliminating errors and outliers. We further devised a method to transform the integrated shear profiles into absolute velocities, and finally we were able to compare the results with simultaneous Pegasus profiles.

The results presented here were from two *Meteor* cruises in the western tropical Atlantic in October 1990 (M14) and May 1991 (M16).

Corresponding author address: Dr. Jürgen Fischer, Institut für Meereskunde an der Universität Kiel, Regional Ozeanographie, Düsternbrooker Weg 20, 2300 Kiel 1, Germany.

© 1993 American Meteorological Society

2. Technical aspects

a. Instrument package

We used a standard 153.6-kHz self-contained ADCP with 20° beam angle and 20-MB EPROM (electronically programmable read only memory) recorder attached to the frame of a 24-bottle rosette and a Neil Brown Mark-III CTD (Fig. 1). Only minor modifications of the rosette frame were necessary to mount the ADCP vertically. The first trials were carried out with a 1400-m pressure case; later, the system was upgraded for 5000-m depth rating. Only two water bottles had to be removed from the rosette frame in favor of the ADCP. The package was lowered with 1 m s^{-1} except during the upward profile when water samples were taken.

b. ADCP parameter settings

The ADCP parameters were set to meet the special requirements of the application; a more detailed parameter list is given in the Appendix. We selected a nominal bin width of 16 m; the depth cell (bin) length for the 20° beam configuration then was 17.36 m from geometric considerations. Every 8 s the mean over 12 individual velocity profiles was stored. This was the highest achievable sampling rate for the 8-s ensemble interval and the prescribed range (18 bins).

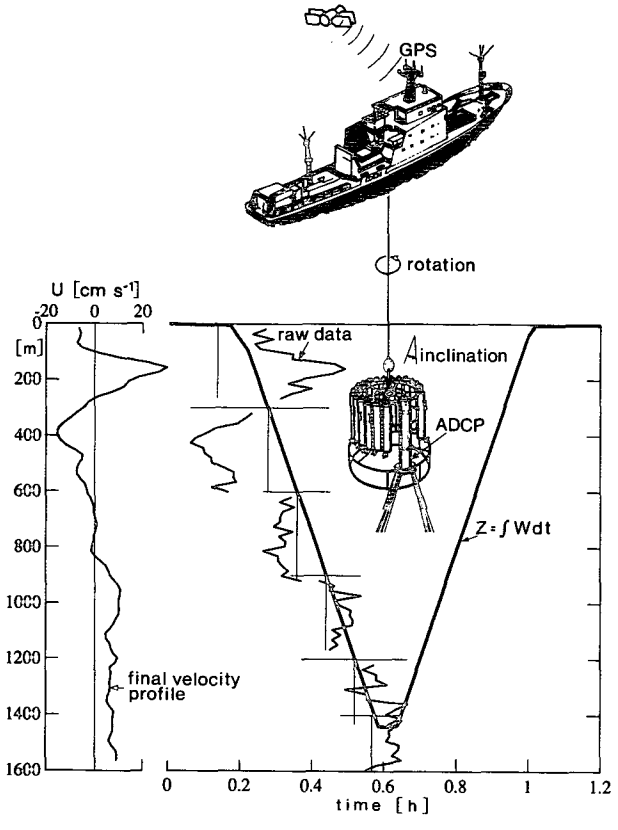

FIG. 1. Measurement scheme with lowered CTD–ADCP instrument package. Motions of the package consist of lowering speed, ship drift, as well as inclination and rotation. Included is a scheme of the depth–time diagram with individual raw velocity profiles and the final absolute velocity profile at M14 station 660.

Good data were obtained over a range of about 300 m (18 bins) close to the surface, but below about 1000 m the range was reduced to less than 8 bins (140 m); a more detailed description of the measurement range is given in the discussion. Data of each profile contain the three velocity components in earth coordinates plus the so-called error velocity. The latter is the difference of the vertical velocity measurements of the two orthogonal beam pairs, while the vertical velocity W is the average of the two.

At a lowering rate of 1 m s^{-1} there were at least two measurements per depth cell, and more when the drop rate was less. In addition to the velocity components, the backscattered energy and quality parameters were recorded. Due to the small number of profiles averaged, the short time inaccuracy of the horizontal velocity data is fairly large; their standard deviation is 2.8 cm s^{-1} (RDI 1989). A typical 4000-m cast consisted of about 1500 ensembles, occupying 550 KB of data storage, and the cast was normally completed within 3 h; that is, there was enough storage space for about 35 profiles before the instrument had to be opened to erase the EPROMs. Battery capacity was sufficient for this number of profiles when using alkaline D-cells (50 cells for the two battery packages). The operating costs are therefore negligible.

c. Behavior of instrument package

Two perpendicular tilt sensors (pendulum potentiometers) measure pitch and roll angles, and ADCP heading is measured by a flux gate compass. The orientation parameters are used to transform the data from beam to earth coordinates. Their means and standard deviations (over 12 measurements) were stored for each ensemble. An example of the behavior of the package is shown for M14 station 660 (Fig. 2). During several phases of the up and down trace both inclinometers show angles up to 6° against the vertical axis, well within the range of proper component decomposition. The important point here is that their standard deviations were small, typically less than 1°, which means that the inclination of the instrument package was changing rather slowly. Averaged over the duration of that cast the mean deviations from the vertical axis were 2° for the pitch angle and 0.5° for roll (Fig. 2). Orientation changes (Fig. 2, "heading") were also slow with standard deviations being normally less than 1°. Close to the surface the motion of the instrument package was more vigorous, and the higher-frequency fluctuations in the orientation parameters corresponded to the ship's roll period. This behavior was typical for the ADCP with the 1400-m pressure case; for the much heavier housing of the 5000-m version the mean tilt was larger. In some of the profiles with

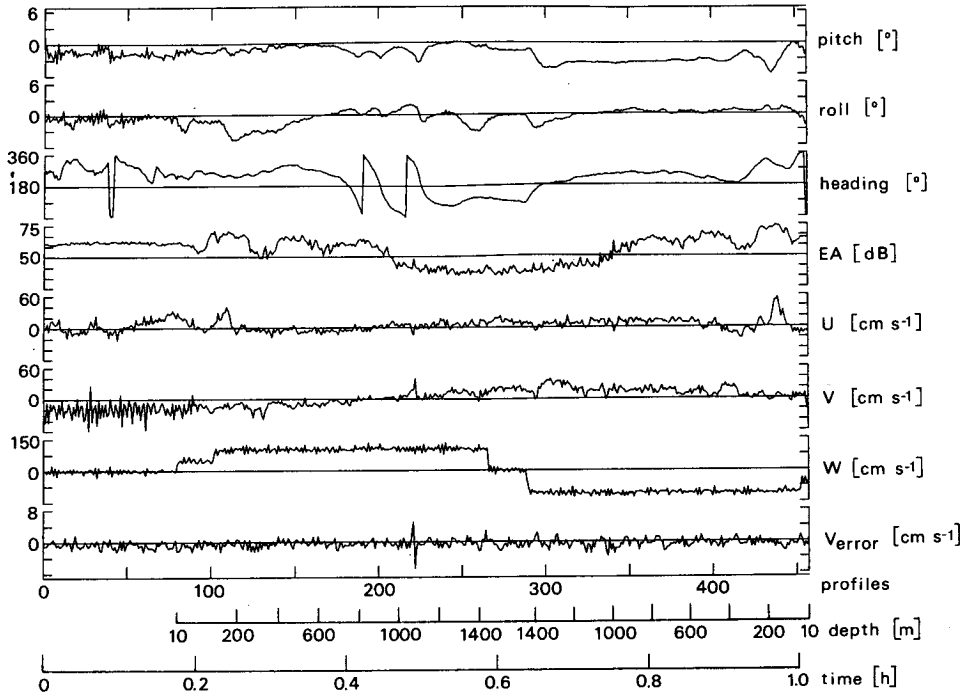

FIG. 2. Raw data measured by the lowered ADCP (M14 station 660). From top to bottom: inclination angles (pitch and roll), true heading, echo amplitude EA, east–west velocity U, north–south velocity V, vertical velocity W, and error velocity V_{err} (all from bin 2). Below the number of profiles, the time and the depth of the cast are shown.

the 5000-m version we observed tilt angles in excess of 15°. The largest tilt angles occurred during the downcasts and at stations with intense surface currents (large ship drift). This behavior could be improved by properly ballasting the instrument package in future experiments.

3. Data processing

The data processing was performed on an IBM-compatible 386 PC with at least 4 MB of memory and a coprocessor. Typically, the final velocity profile was determined within a few minutes of computer time. The processing scheme is summarized in a flow diagram (Fig. 3) showing the different stages from raw data to the final velocity profile. More detailed information about each processing stage is given below.

a. Velocity scaling

The transformation from the raw Doppler frequencies to velocity units depends on the sound speed, which was calculated using the ADCP temperature record; the instrument depth from the integration of the vertical velocity; and constant salinity of 35 psu. Each velocity profile was then scaled by $c(z)/1536$ m s^{-1}, with $c(z)$ the sound speed at depth, and 1536 m s^{-1} the fixed sound speed used in the instrument. In a second step the depth of the instrument was recalculated using the corrected vertical velocities. No sound speed correction was applied to the length of the depth cells. Horizontal currents were rotated according to the magnetic deviation at the location of the station.

b. Bottom detection

This routine was used only for profiles extending down to the bottom, where the bottom reflections occurred as a maximum in the backscattered energy profiles. All data from virtually below the bottom, that is, received later than the bottom reflection, were rejected. At some of the stations the ADCP was lowered very close to the sea floor (less than three bins) yielding a data gap of several minutes duration.

Multiple bottom reflections occurred in conjunction with the high ping rate in discrete depth levels above the bottom. There, the backscattered energy profile showed a pronounced maximum due to the bottom reflection of the acoustic pulse transmitted one ping interval earlier. The depth of the interference layer is determined by

$$Z_{il_n} = Z_{\text{bottom}} - c\Delta t \frac{n}{2}; \quad n = 1, 2, \cdots. \qquad (1)$$

With typical values for the ping rate $\Delta t = 0.5$ s and the sound speed $c = 1500$ m s^{-1}, the first interference oc-

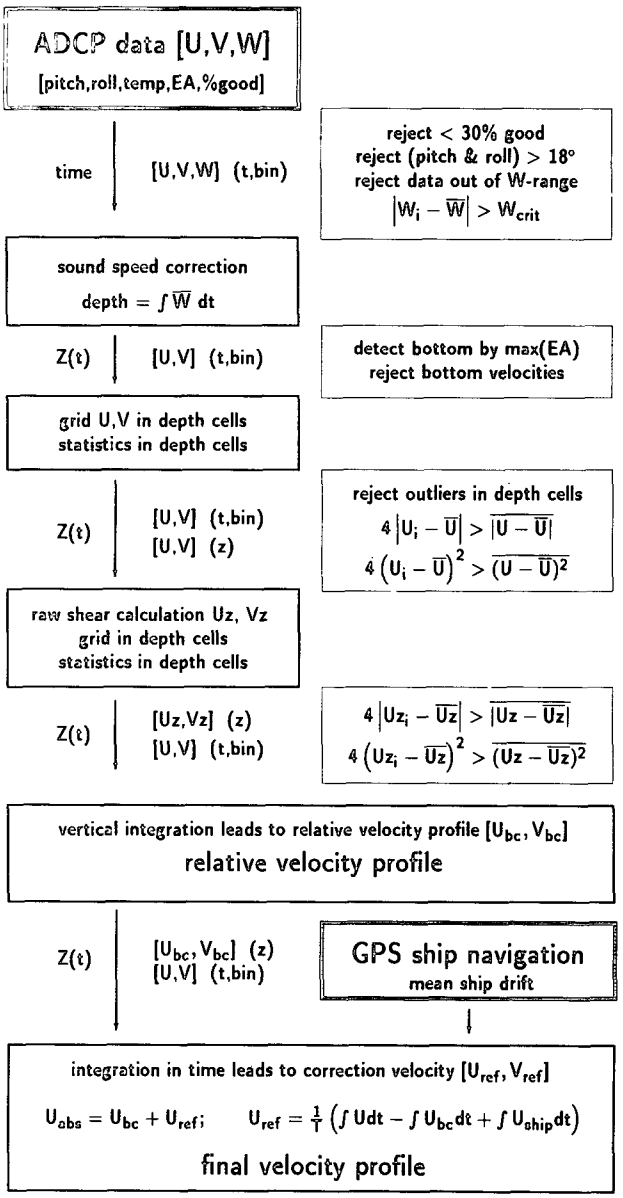

FIG. 3. Data processing flow diagram. Heavy lined boxes show raw input data (ADCP and GPS positions). Medium thick lines are indicative of the main processing algorithms, and thin lines are used for editing routines.

curred about 350 m above the bottom. In some of the cases even a second peak ($n = 2$) could be observed, which results from the bottom reflection of the acoustic pulse transmitted two ping intervals earlier. But, although the backscattered energy in the interference layers was high, most of the horizontal velocities showed no obvious deficiencies compared to adjacent layers. Therefore, we tried to evaluate the data quality by an outlier rejection scheme rather than eliminating a whole layer. This problem could be reduced by using slower or asynchronous ping rates, but the overall velocity accuracy will then be reduced.

c. *Derivation of instrument depth*

Without an internal pressure gauge the instrument depth is a priori unknown. There are two possible ways to tackle this problem. First, the ADCP data might be synchronized with the CTD profile, but time gaps in the CTD record during water-sampling stops prevented us from matching CTD depth and ADCP data. For this reason, and in order to be as independent from other data sources as possible, we decided to use the time-integrated vertical velocity (Fig. 1). The vertical velocity record (Fig. 2, W) clearly shows how the cast was performed. First, with W equal to zero the instrument was held close to the surface; then, it was lowered with 50 cm s^{-1} through the first 100 m, and afterward with 100 cm s^{-1} until the winch stopped at the deepest point of the profile. The upcast of that station was also performed at a rate of 100 cm s^{-1} without any interruptions for water sampling.

Temporal integration of the vertical velocity then gave a time series of the ADCP depth. To obtain the most accurate measure of the drop rate, we averaged W over the range of good data (the procedure to evaluate the range of good data will be described below). A second constraint applied was that the vertical velocity integration over the down- and upcasts should add up to zero. A systematic depth mismatch of about 30 m was typical for a 1400-m-deep profile (100 m for a 4000-m profile). This corresponds to an average vertical velocity bias of -0.9 ± 0.3 cm s^{-1} for 11 ADCP profiles during the M14 cruise. We suspect this bias is due to filter skewness, that is, a systematic instrumental error (Chereskin et al. 1989). Magnitude and sign of the error was consistent with moored ADCP records (Schott et al. 1993), where annual-mean downward velocities of about -0.5 cm s^{-1} were observed in five moored ADCPs. There, the W bias was independent from the view direction of the ADCPs (up- and down-looking) but showed a dependency with respect to bin length. Consequently, the W bias was removed, and a good test for the depth performance is the comparison between the largest CTD depth and the largest ADCP depth. Averaged over 11 profiles of the M14 cruise the depth of the casts agreed within 7 m $\pm$ 10 m, which was sufficient for depth gridding the data with a vertical resolution of one bin (17.36 m).

d. *Raw velocity shears*

The velocity measurements are a combination of the motion of the instrument package and the ocean current (Fig. 2). While the ocean current may change over the range of the ADCP measurements (typically 200 m), the instrument velocity contribution has no vertical shear in an individual profile (ensemble). Therefore, vertical differentiation of the horizontal velocities rejects the unwanted instrumental motion in individual profiles but it also eliminates any mean ocean velocity component.

Shear calculations were done with different differentiation schemes, and the best results in terms of stable mean shears and vertical resolution were obtained by using three-point central differences and subsequent interpolation to a regular depth grid. The effective vertical resolution of the shears is twice the bin length (17.36 m), and a vertical resolution of one bin length chosen for the depth gridding is sufficient.

e. Editing

Velocity errors might arise for various reasons, for example, bottom reflections and strong instrumental accelerations in the near-surface layer (pitch and roll fluctuations, Fig. 2). Those were the obvious errors, but there were also velocity and shear spikes that were detected only by consistency tests. Therefore, we carefully edited the data and eliminated erroneous data during subsequent processing stages rather than rejecting data solely on the basis of the percent good parameter.

First, all velocity data with "percent good" parameter less than 30% were rejected; that is, 30% of the data in a certain ensemble had to exceed the prescribed signal to noise ratio of 6 dB. This is a rather loose constraint compared to the 80% criterion of Firing and Gordon (1990).

Further, all data closer than 24 m to the instrument (6-m blanking delay plus bin 1) and profiles with pitch or roll angles exceeding 18° were rejected.

- The second criterion was based on the fact that the vertical velocity should be constant for an individual profile. The range of valid W data was determined by comparing the vertical velocity of a certain bin with the mean over the preceeding bins. Once the difference between these values exceeded a threshold (5 cm s^{-1}), all velocity data farther away from the ADCP were eliminated. Most of the data rejected by this constraint were from below 1000 m (low-scattering environment).
- After the bottom detection, all data below 35 m (two bins) above the bottom were eliminated.
- We observed large horizontal velocity spikes in individual depth cells, for example, in the bottom interference layers. These should be removed prior to shear calculation and they could not be rejected by a sharper initial "percent good" criterion. The horizontal velocities were gridded to depth cells, and the contributions of the individual traces to each depth cell were edited in two phases. First, a mean absolute difference from the average was calculated, and all data deviating by more than four times the mean difference were eliminated. Large individual spikes were removed in this stage. Second, means and standard deviations were calculated for the remaining data, and all data outside a two-standard-deviation threshold were discarded.
- A similar procedure was applied to the shear values but now for the combined traces. In the upper 1000 m these calculations were done for each depth cell separately; below, adjacent depth cells were included to achieve more stable mean shears. The number of valid data was smaller at depth (due to range reduction) and prevented us from calculating a stable mean shear on the basis of a single depth cell. Thereafter, shear spikes were rejected in the same two steps as described for the raw velocities.

While a significant number of velocities and shears were rejected, there was no indication of an asymmetric distribution of rejected data between down and up trace. Velocity editing removed spurious data in the bottom interference layers. Additionally, there were a few velocity profiles in the near-surface layer rejected, which showed large instrumental motion. Finally, we should mention the large number of bin 2 data rejected, probably an indication of measurement problems close to the ADCP.

f. Mean shears and relative velocities

Subsequent shear profiles should be equal over the overlapping range providing the ocean current does not change in between. Furthermore, we assume that any ocean variability on time scales corresponding to the duration of the cast was small, and we are therefore able to combine up and down traces. The edited shear values were interpolated to the adjacent grid point, and the gridded data were then averaged using the total dataset and the down- and upcast separately. Standard deviations for each of the three mean shear profiles were also calculated. The number of shear contributions M to a depth cell varies with the drop rate W, the range of good measurements (n bins), the ensemble interval (EI = 8 s), and the size of the depth cell (equal to bin length BL); see also Firing and Gordon (1990):

$$M = (n - 2)\frac{\mathrm{BL}}{W\,\mathrm{EI}}. \qquad (2)$$

In the top 1000 m with valid data over 16 bins there were about 30 shear contributions per trace, or 60 per cast. Below that depth, the range and therefore the number of contributions was reduced by roughly a factor of 2. This could be compensated at the cost of ship time by using slower drop rates in the deep ocean.

The mean shear profiles were then vertically integrated to obtain a relative velocity profile.

g. Determination of reference velocities

Absolute velocity profiles may be obtained either by adjusting the vertically integrated shear profile to a known reference velocity or by temporal integration of the ADCP measurements and correction for the ship drift (determined from GPS positioning).

Independent velocity measurements—for example, from a ship-mounted ADCP—could be used to adjust the relative velocity profiles over the top 300 m. During

our first trials the shipboard ADCP was switched off on stations to avoid possible interference between the two ADCPs that were operating at the same frequency. Only very recently we found that this was no problem in praxis. A similar way to determine a reference velocity near the surface is to hold the CTD/ADCP at constant depth at the beginning and/or the end of the cast (Fig. 2). The data from this period should be processed like data from a ship-mounted ADCP; namely, average the profiles and subtract the ship speed relative to the bottom (from GPS positioning).

The bottom-track mode of the ADCP might also be used to obtain a reference velocity close to the bottom. We made no use of the bottom-track mode, because it would reduce the number of profiles per ensemble due to additional bottom-track pulses and subsequently the accuracy of the velocity measurements would be degraded. Instead, we tried to derive the "bottom velocity" from the normal profiling mode, which worked well for tracking ice with moored upward-looking ADCPs. Here, the results were not encouraging. For each ensemble with the bottom in range we subtracted the motion of the ADCP relative to the bottom (bottom velocity) to determine the ocean current in the near-bottom layer. But, the scatter of the remaining velocities was too large to determine a stable mean.

With no shipboard ADCP data available on station, only very short velocity segments before and after the profile could be used for adjustment, and due to the short integration time (a few minutes), the errors might be large (order 5 cm s^{-1}). Nevertheless, for interrupted casts this is probably the only method to get an estimate of the reference velocity.

Our favorite approach to determine the reference velocity uses only the ADCP data and GPS positions at those times when the instrument goes into the water and when it surfaces again. For this method an uninterrupted ADCP record from the beginning to the end of the cast is needed.

The general problem for ADCPs mounted on moving platforms is to remove the motion of the ADCP relative to the bottom in order to get the ocean current. In vessel-mounted applications, the ship speed relative to the bottom can be determined from absolute positioning—for example, GPS. Here, the position of the instrument is unknown, and it is dragged through the water in an unknown manner. But, the motion of the ADCP relative to the bottom can be determined in an integral sense, if only the end positions (e.g., from GPS navigation) of the cast are known.

By splitting the measured velocities into their constituents, we obtain

$$U_{\text{meas}}(t) = U_{\text{ref}} + U_{bc}[z(t)] - U_{\text{ADCP}}(t). \quad (3)$$

Here, U_{ref} is the constant reference velocity and U_{bc} the relative (baroclinic) velocity profile from shear integration. The ADCP motion U_{ADCP} consists of a slowly varying component corresponding to the ship drift (U_{ship}) and the more fluctuating (U_{CTD}) motion of the instrument relative to the ship:

$$U_{\text{ADCP}} = U_{\text{ship}} + U_{\text{CTD}}. \quad (4)$$

When integrating Eq. (4) over the period of the cast T the high-frequency motion U_{CTD} vanishes by definition:

$$U_{\text{ref}} = \frac{1}{T}\left\{-\int U_{bc}[z(t)]dt + \int U_{\text{meas}}(t)dt + dX\right\}. \quad (5)$$

The last term on the right-hand side is

$$dX = \int U_{\text{ADCP}}dt = \int U_{\text{ship}}dt; \quad (6)$$

namely, the distance dX between the two positions of the instrument, which we know to be the accuracy of the positioning system.

We can easily integrate the measured velocity and with good GPS data available we can determine the mean ship drift. Additionally, we need the time integral over the baroclinic velocity. Using $z(t) = \int W(t)dt$ the relative velocity profile $U_{bc}(z)$ can be transformed into a time series of baroclinic velocities.

4. Accuracy considerations

a. Shear statistics

To evaluate the quality of the measurements we compared the shear statistics with theoretical values. For an individual velocity measurement (ensemble average) the short time accuracy can be estimated by the standard deviation (RDI 1989)

$$\sigma_u = \frac{2.4 \times 10^5}{F\text{BL}\sqrt{N}}\ \text{m s}^{-1} = 2.8\ \text{cm s}^{-1}, \quad (7)$$

with N the number of pings per ensemble (12), BL the length of the vertical depth cell (equal to pulse length), and F the frequency of the instrument (153.6 kHz). The corresponding value for shears calculated with central differences is then

$$\sigma_s = \frac{\sqrt{2}\,\sigma_u}{2\text{BL}} = 1.1 \times 10^{-3}\ \text{s}^{-1}. \quad (8)$$

With M shear contributions, typically between 50 and 10 [see Eq. (2)] at a certain grid point, the theoretical standard deviation is in the range of 1.6×10^{-4}–3.6×10^{-4} s^{-1}. Below the intense shear zones close to the surface, the standard deviations of the measured shears were around 10^{-3} s^{-1} (Fig. 4), a factor of 3–5 larger than the theoretical values. In layers with weak shears the standard deviations were even larger than the mean (Fig. 4), but we observed no significant differences between up- and downshear profiles in these layers. At both ends of the profile, standard deviations increase, presumably due to higher shear variability in the top

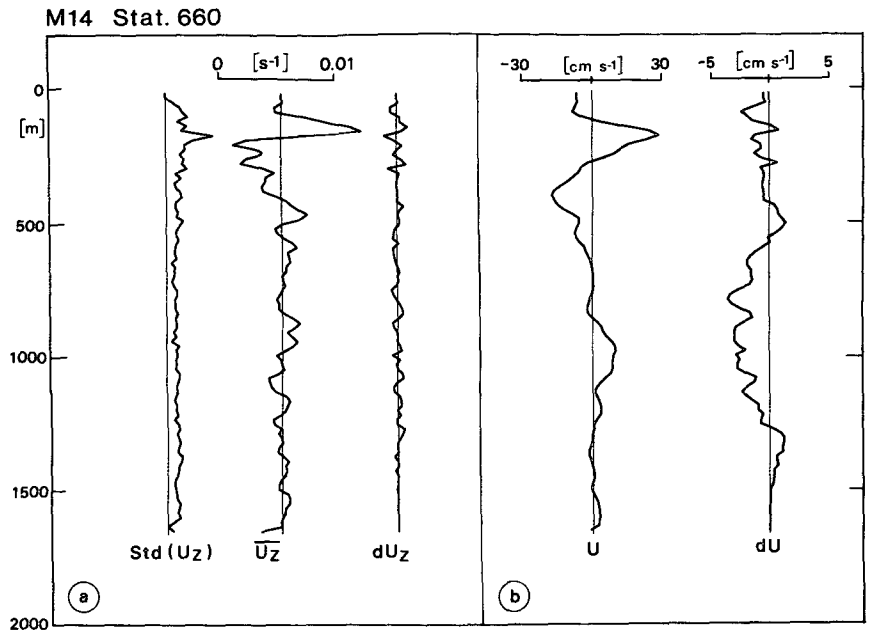

FIG. 4. Mean vertical shear profile of zonal velocity U_z, standard deviation profile of shear std(U_z), and up–down difference of shear dU_z at M14 station 660 (a). Zonal velocity component U (using down- and upcasts simultaneously) and (b) up–down difference dU.

layers and due to range reduction in the deepest parts of the profiles.

b. *Comparison of down- and upcasts*

Only the 1400-m profiles were used for a comparison of the down- and upcasts. For the very deep casts, the reduction in measurement range prevented us from processing the casts separately. All profiles in Fig. 5 were integrated from a common level of 1500 m, and the mean and rms differences between down- and upcasts were calculated from 173 m (ten bins below the surface) downward.

The overall agreement between the individual traces was good. The mean difference for the zonal velocity component varied between -1.3 and 2.4 cm s^{-1}, and rms differences were in the range between 1.8 and 5.2 cm s^{-1}. For longer profiles the expected rms differences will be larger, depending on the ratio of the individual profile range to the total depth range (Firing and Gordon 1990).

The largest rms difference, observed at station 654, resulted from a depth mismatch between down- and upcasts. No attempts have been made to evaluate how much of the observed differences can be attributed to real ocean variability. Similar results were obtained for the meridional velocity component.

c. *Reference velocity*

For each bin measured by the ADCP we obtain one estimate of the reference velocity U_{ref}. If the number of bins with reliable data changes—for example, due to a reduction of scatterers in deeper layers or for profiles lowered very close to the sea floor—the number of estimates reduces to the minimum number of bins available. First, we made a consistency check of the scatter of U_{ref} for the N estimates. Later the results will be compared with Pegasus data.

Estimates of the reference velocity for bins 3–9 are shown in Table 1. The integrals over the measured and baroclinic velocities depend on the bin chosen for the integration. For example, bin 3 uses data between 52 and 1452 m, and the integration over bin 9 data starts from 156 down to 1556 m, thereby scanning different depth levels. At station 660 the integrals varied as much as 7.5 and 5.8 cm s^{-1} for the measured and baroclinic u component, respectively, but the reference velocity was stable within ± 0.6 cm s^{-1}. Even larger variations were found at station 661 where the integrals varied by as much as 15 cm s^{-1}. There, the standard deviation of U_{ref} was ± 1.3 cm s^{-1}.

The immediate result is that the estimate of the correction velocity is stable and that there are no inconsistencies between the measured and the baroclinic velocities. Although U_{ref} may be calculated for each bin (e.g., bin 3), we finally used all reliable data to achieve the most accurate estimate.

This rather small error of the reference velocity will be increased by two effects. First, position inaccuracies of ± 100 m each will increase the error by 4 cm s^{-1} (1400-m profile) or 2 cm s^{-1} for a 4000-m-deep profile. Second, any data gaps due to bottom interference will

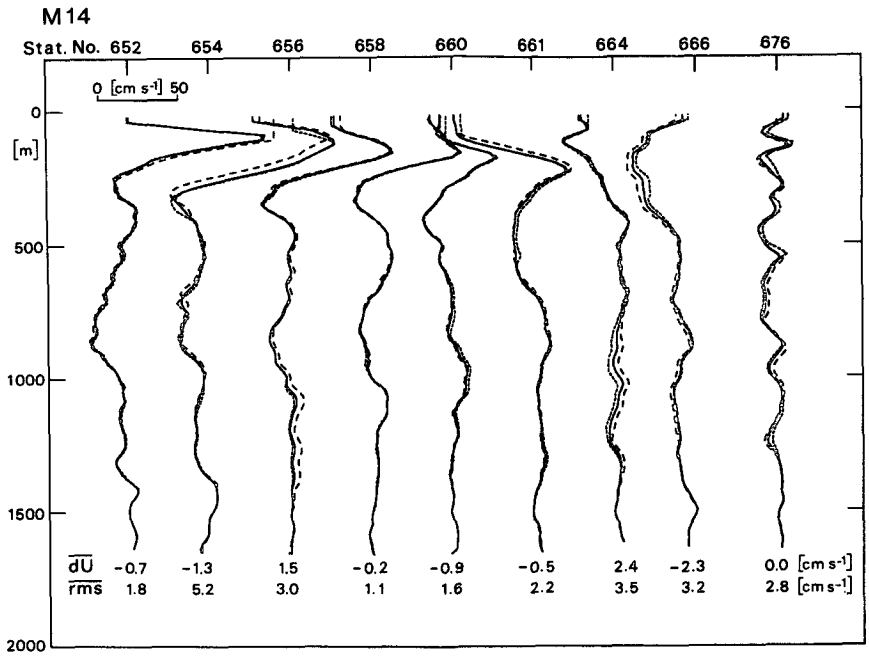

FIG. 5. Zonal velocity profiles offset by 50 cm s^{-1} for 1400-m-deep casts along 35°W. The stations were obtained during *Meteor* cruise M14 from 0.5°N to 5°S. Solid lines are used for the full dataset, dashed for the downcast, and short dashed for the upcast. Below, the mean and rms differences between down- and upcasts are shown (from 173 m downward).

further increase this error. For a gap of 10-min duration in a 4000-m cast (3-h duration) and 20 cm s^{-1} raw velocity another 1 cm s^{-1} may be added to this error. Ignoring the data gap, as we did, is equivalent to integrating the mean ship drift and assuming zero ocean current. The crucial factor is the ratio of the gap interval to the duration of the cast, which has to be reduced as much as possible (short bottom stops).

An independent quality test of the ADCP profiles and the reference velocities was obtained by comparing them with Pegasus velocities at the same stations (U. Send 1992, personal communication). Overall, there was good agreement between the two measurements; Figs. 6a,b shows the Pegasus up- and downcasts at M16 station 291 with the corresponding ADCP profile. The vertical resolution of the two instruments was similar.

TABLE 1. Reference velocity. Station 660: $U_{ship} = -3.1$ cm s^{-1}; $V_{ship} = 2.1$ cm s^{-1}

Bin	U_{meas} (cm s^{-1})	$-U_{bc}$ (cm s^{-1})	U_{ref} (cm s^{-1})	V_{meas} (cm s^{-1})	$-V_{bc}$ (cm s^{-1})	V_{ref} (cm s^{-1})
3	4.4	6.8	8.1	0.4	8.2	10.7
4	5.0	6.6	8.5	−0.1	8.1	10.2
5	4.5	6.7	8.0	0.5	8.0	10.6
6	5.9	6.3	9.0	−1.4	8.7	9.4
7	7.3	4.9	9.0	−1.5	9.6	10.2
8	8.7	3.3	8.9	−1.3	9.6	10.4
9	11.9	1.0	9.8	−1.1	9.4	10.5
3–9	$U_{ref} = 8.8 \pm 0.6$ cm s^{-1}			$V_{ref} = 10.3 \pm 0.4$ cm s^{-1}		

Due to the central differences, the ADCP data were smoothed over two bins (36 m) and the Pegasus data were low passed approximately over the same range.

The statistical correspondence between the two measurements is summarized in Table 2 for all deep (3000–4500 m) stations and the depth interval from 100 m below the surface to 100 m above the bottom. The mean difference between Pegasus up- and downcasts lies in the range of −1.3–2.2 cm s^{-1}, and the rms difference is about 3 cm s^{-1}. Both the mean and the rms difference between Pegasus downcast and the full ADCP profile were somewhat larger (Table 2). On average (over the ten stations), the rms difference was 5.1 cm s^{-1} for the zonal component and 4.8 cm s^{-1} for the meridional component. The largest deviations were found for profiles 293 and 306 but only in one of the velocity components. At these stations the ADCP profile showed an offset with respect to the Pegasus data, suggesting problems in the determination of the reference velocity. This is supported by the smaller standard deviations of 4.5 cm s^{-1} (station 293 U component) and 4.8 cm s^{-1} (station 306 U component) compared to the rms differences. Standard deviations and rms differences were about the same for the V components.

5. Discussion

A 153.6-kHz self-contained ADCP was lowered together with a CTD attached to the frame of a 24-bottle

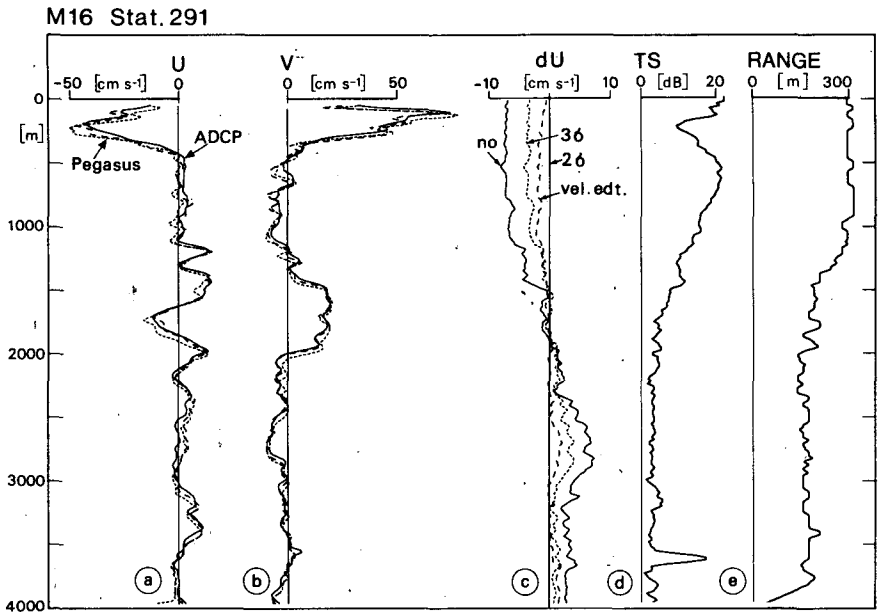

FIG. 6. ADCP and Pegasus velocity profiles at M16 station 291 and (a) and (b). ADCP velocities are plotted solid, Pegasus downcast is dashed, and Pegasus upcast is short dashed. Velocity difference to the final profile for different editing stages (c). The right-hand sides (d) and (e) show the profile of the relative target strength (TS) together with the range of good-quality data at the same station.

rosette sampler. After elimination of the unknown instrumental motion and the rejection of unreliable data, mean shear profiles over full ocean depth were obtained. Vertical integration of the shear profiles led to relative velocity profiles, and a method was proposed to convert relative to absolute velocities using GPS ship positioning. For the 1400-m profiles, the errors—evaluated from up–down comparison—were much smaller than those found by Firing and Gordon (1990). Technically, there were two obvious differences between the two studies, the ADCP frequency and the data processing method. The 300-kHz system used by Firing and Gordon (1990) is supposed to have higher accuracy but has less range than the 153.6-kHz system we used, and the authors expected the accuracy of the 300-kHz ADCP to be higher at high vertical wavenumbers and about equal at low wavenumbers. But, the shear standard deviations seemed more similar than expected from theory (E. Firing 1993, personal communication), and the better performance within the upper 1400 m might be a result of the larger ranges obtained with the 150-kHz system. Farther down, the ranges of the two instruments were more similar, and we therefore expect the improved performance to be the result of the data processing scheme. Editing is the most essential part in the prescribed processing. Imagine, the mean shear in a certain depth cell is biased by the order of the shear standard deviation (10^{-3} s^{-1}), then the vertical integration would show a 1.7 cm s^{-1} velocity offset (depth cell length is 17.36 m) of the layer above the erroneous value compared to below. Thus, undetected spikes in shears contribute to the red part of the wavenumber spectrum. A few such spikes could distort the velocity profiles by several centimeters per second, and the result would be a velocity profile in which the high wavenumber part is reasonable while the lower wavenumbers are distorted in an unpredictable manner. Large up–down differences were typical for unedited profiles, and it might well be that this effect was observed by Firing and Gordon (1990), Fig. 3.

An example of how editing influences the velocity profile (U component of M16 station 291) is illustrated in Fig. 6c. The largest difference compared to the final velocity profile is obtained by the no-editing case, with

TABLE 2. ADCP vs Pegasus stastistics.

	Pegasus down − Pegasus up				ADCP − Pegasus down			
	U component (cm s^{-1})		V component (cm s^{-1})		U component (cm s^{-1})		V component (cm s^{-1})	
Station	Mean	rms	Mean	rms	Mean	rms	Mean	rms
289	0.7	5.1	−0.2	3.7	1.6	5.5	−0.4	5.2
291	1.1	2.9	−1.0	3.1	−1.0	4.8	0.4	3.3
293	−0.4	3.5	−1.0	4.6	4.3	6.2	−0.1	5.5
295	−0.7	2.2	1.0	2.3	1.9	6.1	−1.7	4.0
297	2.2	3.2	0.3	4.1	−2.7	5.9	−2.2	5.8
306	0.2	2.1	−0.5	1.6	3.4	5.8	1.5	6.9
310	−1.5	2.9	1.2	2.8	0.2	4.1	−0.9	3.1
313	−0.2	5.5	0.0	4.6	1.0	4.8	−0.5	4.9
316	−0.3	1.8	1.3	2.3	−0.4	4.8	−0.8	4.4
318	−1.3	3.3	1.1	2.5	−0.8	3.3	−0.8	5.0

the top layers deviating by about 7 cm s^{-1} toward negative U and with a positive deviation of similar magnitude in the lower layers. Velocity editing alone had a big effect: the deviations decreased to less than ±3 cm s^{-1}. Velocity plus shear editing with a three-standard-deviation threshold showed a tendency to reduce the deviations, but the best overall performance was achieved with the prescribed editing scheme (two-standard-deviation threshold).

The method to determine the unknown reference velocity worked fairly well, provided there was an uninterrupted ADCP time series and good GPS data quality. Then, the reference velocity may be as accurate as 2 cm s^{-1} (Table 1 and Figs. 6a,b). Any interruption of the time series, for example, if the instrument is lowered very close to the bottom (less than three bins), might degrade the accuracy of the reference velocity to about 5 cm s^{-1}. The comparison of the depth determined from the W integration and the CTD depth shows that after a linear correction of the bias there is no need to merge CTD data into the ADCP measurements, and those interested only in the velocity measurements may lower the ADCP without the CTD on any hydrographic wire.

What are the limitations of the method? Problems occurred after several deep casts with water leaking through a broken transducer. New transducers were implemented and survived several stations down to 2500 m in the Mediterranean Sea.

One obvious deficiency of the deep casts was the reduction in range observed both in the deeper levels of the tropical Atlantic Ocean (Fig. 6e) and in the western Mediterranean. This is due to a reduction of the signal-to-noise ratio as can be deduced from the profile of the target strength (TS) (Fig. 6d) relative to a prescribed source level (Urick 1983). In general we observed high TS values within the top 1000 m, and within the bottom interference layer, here 3700 m in depth (Fig. 6d). Below about 1000 m, the TS decreases to a level about 20 dB lower than the surface value. This could either be due to a reduction of the ADCP source level with depth or due to the lack of scatterers in the deeper layers. The manufacturer was not able to perform a source-level calibration under high pressure, which should help to identify the reason for this behavior. We also found some indications of a TS hysteresis between down- and upcasts in the deep layers, which almost certainly was instrumental.

Concluding, the lowered ADCP is a valuable tool to measure ocean deep velocity profiles. To improve the performance of the lowered ADCP application, further technical improvements regarding measurement range and ping-to-ping accuracy are required; here we expect some progress with the new broadband ADCP technology.

Acknowledgments. We thank Uwe Send for making the Pegasus system operational and for many helpful discussions. We appreciate many helpful suggestions from Fritz Schott, and the technical support by Claus Meinke and Uwe Papenburg. We would also like to thank Jörg Reppin who operated the ADCP during the M16 cruise. We further appreciate helpful comments by E. Firing and the anonymous reviewers.

APPENDIX

ADCP Parameters

For potential users of the lowered ADCP application, a list of the specified parameters is provided in Table A1. We explicitly note the very important transformation of the velocities into earth coordinates prior to ensemble averaging. Each ensemble should also contain "percent good" and "echo amplitude."

TABLE A1. ADCP parameter setting.

Parameter	Value	Meaning
I	16	Transmit interval in meters (equal to bin length)
J	60	Blank after transmit in 0.1 m
L	4	Bin length—2^L m (nominal)
M	30	Ensemble percent-good data
N	60	Signal to noise threshold for good data in 0.1 dB
P	12	Number of pings per ensemble
Q	18	Number of depth cells (bins)
R	800	Time between ensembles (8 s)
V	—	Time between pings (maximum sampling rate)

REFERENCES

Chereskin, T. K., E. Firing, and J. A. Gast, 1989: Identifying and screening filter skew and noise bias in acoustic Doppler current profiler measurements. *J. Atmos. Oceanic Technol.*, **6**, 1040–1054.

Firing, E., and R. Gordon, 1990: Deep ocean acoustic Doppler current profiling. *Proc. IEEE Fourth Working Conf. on Current Measurements*, Clinton, MD, Current Measurement Technology Committee of the Oceanic Engineering Society. 192–201.

Joyce, T. M., D. S. Bitterman, and K. E. Prada, 1982: Shipboard acoustic profiling of upper ocean currents. *Deep-Sea Res.*, **29**, 903–913.

Luyten, J. R., B. Needell, and J. Thompson, 1982: An acoustic dropsonde—Design, performance and evaluation. *Deep-Sea Res.*, **29**, 499–524.

RDI, 1989: *Acoustic Doppler Current Profilers—Principles of Operation: A Practical Primer.* RD Instruments, 36 pp.

Schott, F., 1986: Medium-range vertical acoustic Doppler current profiling from submerged buoys. *Deep-Sea Res.*, **33**, 1279–1292.

——, K. Leaman, and R. Zika, 1988: Deep mixing in the Gulf of Lions, revisited. *Geophys. Res. Lett.*, **15**, 800–803.

——, M. Visbeck, and J. Fischer, 1993: Observations of vertical currents and convection in the central Greenland Sea during the winter of 1988/89. *J. Geophys. Res.*, in press.

Spain, P. F., D. L. Dorson, and H. T. Rossby, 1981: Pegasus: A simple, acoustically tracked velocity profiler. *Deep-Sea Res.*, **28A**, 1553–1567.

Urick, R. J., 1983: *Principles of Underwater Sound.* McGraw-Hill Book Company, 423 pp.